CMOS Compatible Fully Integrated Mach–Zehnder Interferometer in SOI Technology

P. Dainesi, A. Küng, M. Chabloz, A. Lagos, Ph. Flückiger, A. Ionescu, P. Fazan, M. Declerq, Ph. Renaud, and Ph. Robert

***Abstract*—We present a fully integrated Mach–Zehnder interferometer in silicon-on-insulator technology. Modulation of the index of refraction is achieved through the plasma dispersion effect resulting in a bandwidth in the 10 MHz range. A particular and innovative design makes this device completely compatible with CMOS technology allowing electronic functions to be integrated on the same substrate. Measurement results, limitations due to thermooptic effect and absorption related to charge injection together with further improvements are discussed.**

***Index Terms*—CMOS, Mach–Zehnder, plasma dispersion, SOI optoelectronics, thermooptic effect.**

SILICON waveguides in silicon-on-insulator (SOI) technology have been the subject of much investigation in the past years due to their high potentiality in optoloelectronic circuits [1]–[2]. Silicon is presently the most exploited and well-known medium for integrated electronics, but it is also highly transparent in the infrared spectral region enabling low-loss optical waveguiding. Light sources in plain crystalline silicon are not achievable, as well as detectors in the infrared spectral region. Recently, to overcome this problem research has been started on Er-doped porous silicon for light emission, amplification and detection [5], [6], and metal-semiconductor–metal for light detection [7], making out of SOI a very promising technology. Hybrid integrations with Si–Ge heterostructures have also been proposed [4] and achieved. Pockels effect being absent in silicon, all other possible phase modulation techniques have been investigated: Franz–Keldisch effect, Kerr effect, charge carrier effect (also known as plasma dispersion effect), and thermooptic effect. The first two have been calculated in [8] and have shown very low efficiency. Plasma dispersion effect has also been investigated [8] and is the most promising effect. Thermooptic effect has also been extensively investigated and a linear dependency of the index of refraction versus temperature has been shown in [11].

Manuscript received December 6, 1999; revised March 3, 2000.

P. Dainesi, A. Küng, and Ph. Robert are with the EPFL, Swiss Federal Institute of Technology, Laboratoire de Métrologie, 1015 Lausanne, Switzerland.

M. Chabloz was with EPFL, Swiss Federal Institute of Technology, Institut de Microsystèmes, 1015 Lausanne, Switzerland. He is now with Mitsubishi Electric Corporation, Advanced Technology R&D Center, Microsensors Group, Japan.

A. Lagos was with the EPFL, Swiss Federal Institute of Technology, Institut de Microsystèmes. He is now with the CSEM, Centre Suisse d'Electronique et de Microtechnique, SA Jaquet-Droz 1CH-2007 Neuchatel, Switzerland.

P. Flückiger and P. Renaud are with the EPFL, Swiss Federal Institute of Technology, Centre de Microtechnologie, 1015 Lausanne, Switzerland.

A. Ionescu, P. Fazan and M. Declerq are with the EPFL, Swiss Federal Institute of Technology, Laboratoire d'Électronique Générale, 1015 Lausanne, Switzerland.

Publisher Item Identifier S 1041-1135(00)04611-5.

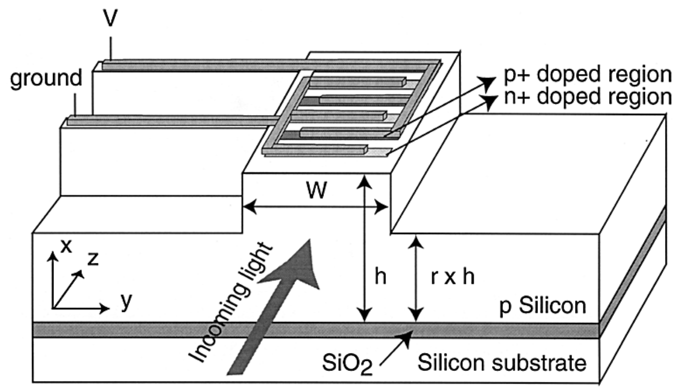

Fig. 1. SOI rib waveguide. Schematic view of the presented phase modulator with longitudinal contacts integrated on top of the waveguide rib.

We present the first, to our knowledge, fully integrated Mach–Zehnder interferometer in SOI technology designed to be fully compatible with CMOS technology and using plasma dispersion effect for light modulation. Plasma dispersion effect and thermooptic effect will be discussed in this letter in relation with our device, together with further improvements and possible applications.

The structure required for light confinement is the rib waveguide presented in Fig. 1. As it has already been shown in literature [3], [10] a proper choice of the geometrical dimensions can give rise to single mode propagation even for wide waveguides (in the micrometer scale). The insulating layer can be fabricated with different techniques [9]; we have chosen a substrate in separation by implantation of oxygen (SIMOX) technology. Calculated overlap integral of the fundamental waveguide mode with the LP_{01} mode of a standard optical fiber resulted in a best coupling efficiency up to 92% for $W = 10\ \mu$m, $h = 10\ \mu$m, and $r = 0.6$. (see Fig. 1). These are the dimensions chosen for our device, choice that fulfills also the singlemode propagation condition. We measured fiber-to-fiber losses of a simple straight waveguide without any electronics to evaluate propagation losses in silicon and found a value of about 1.5 dB/cm at $\lambda = 1300$ nm. Though this result is far from the best reported, it is still in the range of possible values shown in [9] for a SOI prepared with SIMOX technology but can be improved to 0.2 dB/cm using a bond and etch back SOI (BESOI) substrate.

The arrangement for a phase modulator is shown in Fig. 1; electronic diodes are integrated on top of the optical waveguide. This longitudinal arrangement has a unique advantage over the typical lateral approach seen in all other publications. The

1041–1135/00$10.00 © 2000 IEEE

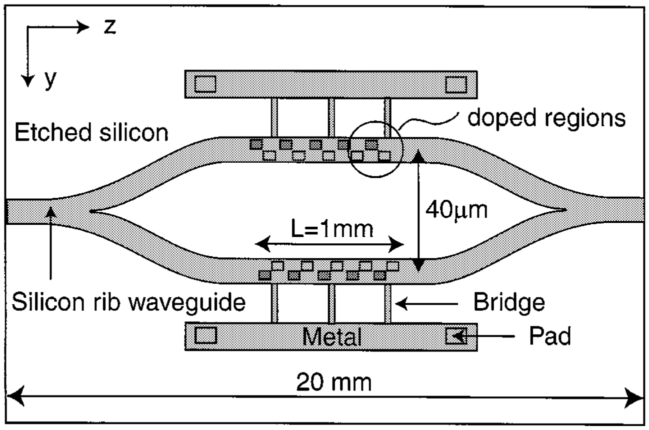

Fig. 2. Schematic top view of the fully integrated Mach–Zehnder interferometer achieved in this work. Electronics are integrated on both arms of the modulator to allow push–pull operation.

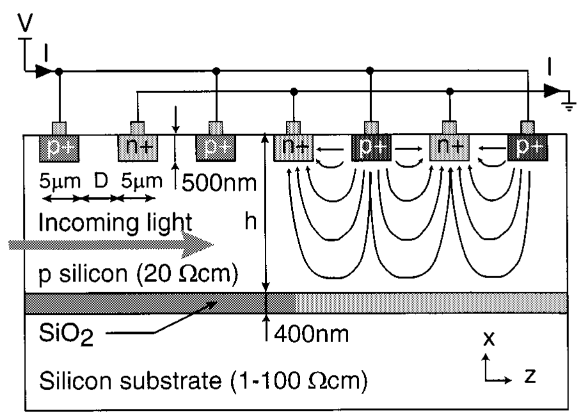

Fig. 3. Cut view along the section of the phase modulator waveguide. Integrated doped regions and current flow are indicated.

major one is that the diodes, doped regions, and contacts, being on the same plane, are fully compatible with CMOS technology, reducing the etching of optical waveguides to a simple and low-cost post processing to the standard electronic integration. Diode pairs connected in parallel, instead of a single lateral diode all along the waveguide structure allow also much more uniform injection of charge. Silicon “bridges” are necessary to support the metal stripes connecting the diodes. Fig. 2 shows a top view of the structure where the bridges are clearly visible though out of scale for obvious reasons. We performed a measurement and found losses due to bridges as well as doped region to be lower than the setup sensitivity. Fig. 3 shows a longitudinal cut view of the phase modulator. The distance between doped regions has been kept large enough ($>10\ \lambda_0/n$ with $\lambda_0 = 1.3\ \mu$m and $n = 3.5$) and has been made quasiperiodic in order to prevent possible formation of Bragg refractors. Simulation studies have been performed using software MEDICI and predicted the possibility for charges to propagate down to the bottom of the guide thus assuring an excellent homogeneity of the injected charge distribution.

Let examine now what ideal change is theoretically predictable for the plasma dispersion effect. The dependency of the index of refraction Δn versus charge injection or depletion (at 1300 nm) is [4], [8]

$$\Delta n = 6.2 \cdot 10^{-22} \Delta N_e + 6 \cdot 10^{-18} \Delta N_h^{0.8} \tag{1}$$

where ΔN_e and ΔN_h are the carrier densities for electrons and holes, respectively. Admitting $\Delta N_e = \Delta N_h = \Delta N$, it is easy to calculate that a $\Delta N = 2.5 \cdot 10^{17}$ cm^{-3} is needed to obtain a π phase shift over 1 mm of propagation. From Hall theory, considering the p+-intrinsic-n+ (PiN) diode structure in Fig. 3 we know that the current density J is given by

$$J = \frac{\Delta N q d}{t_{\text{eff}}} \tag{2}$$

where

- t_{eff} is the average lifetime of charges (50 ns);
- q is the elementary charge unit;
- d is the distance between the diode doped regions.

For our case as the charges flow trough the whole waveguide section we calculated d as the average path, which is $(D + D + 5\ \mu\text{m} + 2(h - 1\ \mu\text{m}))/2$, where D is the distance between the contacts pair. Since $h = 10\ \mu$m and taking $D = 10\ \mu$m we obtain $d = 19.5\ \mu$m leading to $J = 1960$ A/cm^2. The current driven by each diode is then $I = 2.058$ mA. Replicating this structure along 1 mm means heaving 66 diodes for a total driven current of $I_{tot} = 136$ mA. Then for such a device the theoretical phase shift efficiency due to plasma dispersion effect relative to length and current is

$$\eta_{\text{plasma, th}} = \frac{\pi}{I_{\text{tot}} L} = 7.36\pi \cdot \text{A}^{-1} \cdot \text{mm}^{-1}. \tag{3}$$

Concerning thermooptic effect, from theory it is known that an index of refraction variation of $\Delta n_{\text{toe}} = 1.86 \cdot 10^{-4} K^{-1}$ arises from a temperature variation. Power dissipation in the diodes implies a temperature variation according to the following well-known relation:

$$Q = \frac{kA\Delta T}{h} \tag{4}$$

where

- Q is the power dissipated in the waveguide;
- k is thermal conductivity;
- h is the waveguide height;
- A is the area of the cross section;
- ΔT is the temperature variation.

As the thermal conductivity of SiO_2 is about 100 times less than that of Si it is clear that for our dimensions the temperature gradient in the thin SiO_2 layer will be four times greater than that in the Si rib. For simplicity we assumed that the substrate is so big and so highly conductive that the bottom of the SiO_2 layer is at ambient temperature (300 K). Then we discretized the structure of Fig. 1 and calculated an equivalent resistive model. Assuming $Q = 200$ mW we calculated a temperature increase of 1.66 K at the center of the waveguide. This yields to a phase shift due to thermooptic effect of 0.458 π.

A measurement of the normalized output transmitted intensity is shown in Fig. 4. This device is designed as shown in Fig. 2 and contains five bridges driving 15 diodes each for a total of 75 diodes. The length of the phase modulator is $L = 1.11$ mm. During the measurement we did not perform

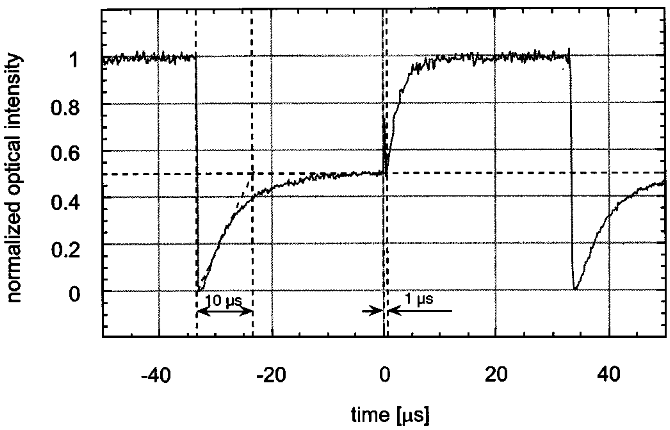

Fig. 4. Normalized intensity at the output of a Mach–Zehnder interferometer driven using a 100-mA square current signal at a 15-kHz rate. Output intensity is one and zero applied current. Contributions of the index changes due to thermal and carrier effect can be distinguished.

push–pull operation by leaving one of the two arms open. It is very easy in the figure to distinguish between the plasma dispersion effect and the thermooptic effect using their respective rise times. A measurement was performed on a single waveguide with a 1-mm-long metal layer on top. In this case, only a thermal phase modulation is present and the bandwidth for the thermooptic effect was measured to be 100 kHz, which is in agreement with the rise time of Fig. 4. As an injection of charge is always associated to power dissipation, a phase modulator based only on plasma dispersion effect is not feasible and thermooptic effect will always be present. In Fig. 4, it is also clear that plasma dispersion effect and thermooptic effect have opposite sign as theoretically predicted.

The injected current for a π phase shift was $I_{\rm tot} = 102$ mA which yields to a measured plasma dispersion effect efficiency relative to current and length of:

$$\eta_{\rm plasma,meas} = \frac{\pi}{I_{\rm tot}L} = 8.83\pi \cdot {\rm A}^{-1}{\rm mm}^{-1}. \tag{5}$$

We measured a bandwidth of the plasma dispersion effect greater than 10 MHz corresponding to a 35-ns switching time, being limited by the current source used for measurements at higher frequencies. In the same Fig. 4 a 0.5-π phase shift due to the thermooptic effect is observable. The voltage drop necessary to inject the 102 mA mentioned above is 2.06 V which gives a thermal dissipated power of about 210 mW.

Both these results are in good agreement with the theoretical model presented above. But the measured 2.06-V voltage drop is higher than the 0.85-V value predicted with MEDICI simulations. This means that the surface integrated diodes show an internal resistance higher than predicted thus increasing the negative influence of thermooptic effect on the device. Electrical tests on the diodes confirmed this observation. focused ion beam (FIB) analysis performed on our samples found an integration problem in the p+ contact, probably due to an incorrect structuring of the metal layer. It is thus realistic to predict a much weaker stray effect due to thermooptic effect.

The insertion (fiber-to-fiber) loss of the device is about 8.5 dB. It must be pointed out that the 3.2-dB Frenell losses can be reduced with the use of antireflection coating and the 3-dB propagation losses can be lowered down to 0.4 dB using a BESOI substrate.

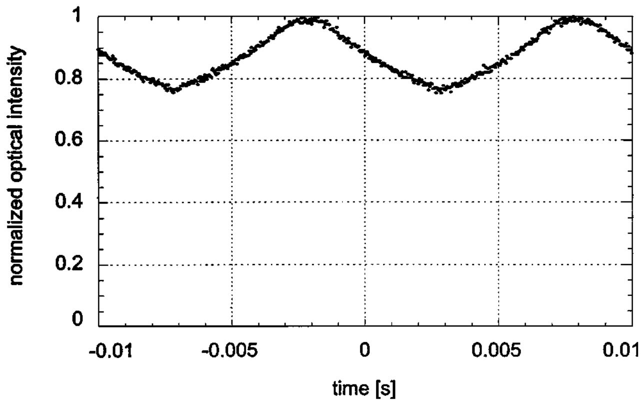

Fig. 5. Normalized intensity at the output of a phase modulator driven using a 150-mA triangular current signal at a 100-Hz rate, showing the effect of carrier absorption.

Fig. 5 shows the measurement of the intensity at the output of a simple straight phase modulator driven by a triangular current signal of 150 mA at a 100-Hz rate. It is clear that 25% of the input intensity is lost due to absorption in the modulation. This measurement is in good agreement with the theoretical study reported in [8] and shows that any phase modulation produced by the plasma dispersion effect induces an optical absorption as expressed by the Kramers–Kronig relation.

In conclusion, we have presented an innovative design for integration of optoelectronic devices in SOI technology applied to a Mach–Zehnder interferometer. Full compatibility with CMOS electronics is achieved and the use of plasma dispersion effect allows a bandwidth larger than standard thermooptic devices. High phase shift efficiency has also been demonstrated.

References

[1] R. A. Soref and J. P. Lorenzo, “All-silicon active and passive guided-wave components for $\lambda = 1.3$ and 1.6 μm,” *IEEE J. Quantum Electron.*, vol. QE-22, pp. 873–879, June 1986.
[2] B. N. Kurdi and D. G. Hall, “Optical waveguides in oxygen-implanted buried-oxide silicon-on-insulator structures,” *Opt. Lett.*, vol. 13, no. 2, pp. 175–177, 1988.
[3] A. G. Rickman, G. T. Reed, and F. Namavar, “Silicon-on-insulator otical rib waveguide loss and mode characteristics,” *J. Lightwave Technol.*, vol. 12, pp. 1771–1776, Oct. 1994.
[4] B. Schüppert, J. Schmidtchen, A. Splett, U. Fischer, T. Zinke, R. Moosburger, and K. Petermann, “Integrated optics in silicon and SiGe-heterostructures,” *J. Lightwave Technol.*, vol. 14, pp. 2311–2323, Oct. 1996.
[5] G. T. Reed and A. K. Kewell, “Erbium-doped silicon and porous silicon for optoelectronics,” *Mat. Sci. Eng. B-40*, pp. 207–215, 1996.
[6] F. Namavar, F. Lu, C. H. Perry, A. Cremins, N. M. Kalkhoran, J. T. Daly, and R. A. Soref, “Er-implanted porous silicon: A novel material for Si-based infrared LEDs,” in *Proc. Mater. Res. Soc. Symp.*, vol. 358, 1995, pp. 375–380.
[7] C. Buchal, M. Löken, and M. Siegert, “Silicon based optoelectronics,” in *Proc. Mater. Res. Soc. Symp.*, vol. 486, 1998, pp. 3–19.
[8] R. A. Soref and B. Bennett, “Electrooptical effects in silicon,” *IEEE J. Quantum Electron.*, vol. QE-23, pp. 123–129, Jan. 1987.
[9] B. Schüppert and K. Petermann, “Integrated optic devices in silicon and silicon-on-insulator materials,” in *Proc. Mater. Res. Soc. Symp.*, vol. 486, 1998, pp. 33–44.
[10] C. K. Tang, G. T. Reed, A. J. Walton, and A. G. Rickman, “Low loss, single-mode, optical phase modulator in SIMOX material,” *J. Lightwave Technol.*, vol. 12, no. 8, pp. 1394–1400, 1994.
[11] C. K. Tang and G. T. Reed, “Higly efficient optical phase modulator in SOI waveguides,” *Electron. Lett.*, vol. 31, no. 6, pp. 451–452, 1995.